

# 4

## *Flexible approach to design PdNPs assembled functional alcoxysilane modified microscaled carrier to facilitate homogeneous enzyme loading*

---

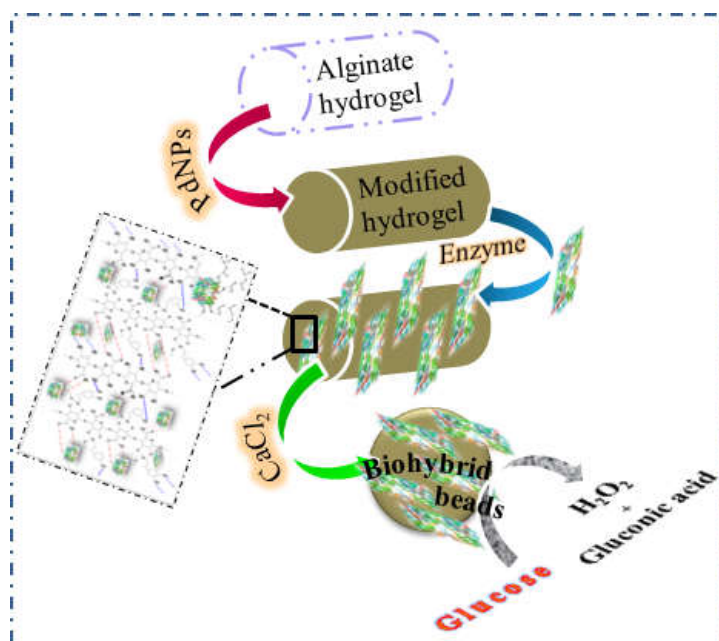
### 4.1. INTRODUCTION

The artificially designed biocompatible enzyme carrier systems are an effective therapeutic tool for diagnostic purposes. Challenge lies in designing such materials which offer the controlled encapsulation of the enzyme molecules and simultaneously allows the significant exposure to substrate molecules. Recently a number of platforms for the encapsulation of proteins have been developed, such as polymer capsules (Johnston et al., 2006; Quinn et al., 2007) synthetic liposomes, (Torchilin et al., 2005) nanohybrid mesoporous Au-SiO<sub>2</sub> based carriers, (Lin et al., 2013) nanogels, (Peng et al., 2016) sol-gel materials (Reetz et al., 1995; Reetz et al., 1996), and also the hydrogels have widespread application in immobilization of macromolecular freight (Hoffman, 2012; Vashisht et al., 2014). Alginate hydrogel possess the required structural integrity which is well suited to immobilization. However, it has the tendency to undergo swelling gradually, as a function of factors like distribution of alternating  $\beta$ -D-mannuronic acid (M) and  $\alpha$ -L-guluronic acid (G) segments, (Batchelor et al., 2012) concentration of calcium, type of solvent added, etc., which reduces its efficiency to encapsulate the

macromolecular materials. The swelling behavior has been investigated thoroughly during recent years (Richardson et al., 2004; Roger et al., 2006). In general, the swelling capacity is determined by chemical potential gradient across the gel particle (Draget et al., 1996). The alginate polymer becomes highly hydrophilic on ionic cross-linking with multivalent cations like  $\text{Ca}^{2+}$ , some fractions may become soluble during the swelling process and evidently leak out of the gel particle (Draget et al., 1996). This phenomenon also regulates the ease of immobilizing the macromolecular cargo into the alginate matrix, as the order of porosity of these hydrogels gets altered on swelling (Jagur Grodzinski et al., 2010).

In this chapter, surface modification of alginate hydrogel in order to construct a stabilized and tunable system for the encapsulation of enzyme has been demonstrated. Alkoxysilane functionalized palladium nanoparticle dispersion (PdNPs) is introduced into the polysaccharide skeleton of alginate hydrogel (Scheme 4.1) for designing the robust enzyme carrier system with nanoscaled pore channels, which is clearly visualised from the SEM micrographs. The lipophilic domain of the alkoxysilane furnishes the active sites for cross-linking with alginate polymer via sol-gel processing (Si – O – Si bridges). The controlled attachment of the residual hydroxyl groups (–OH) of polysaccharide chain with silanol moieties (Si–OH) of alkoxysilane, generates the sol-gel framework with high mechanical stability, as understood by rheological studies (Avnir et al., 2006). It was further claimed that high molecular weight or increased viscosity of the gel promotes flexibility and rapid relaxation, which further promotes the contraction of gel and a high degree of syneresis (Draget et al., 2001). In this chapter it is suggested that the controlled

cross-linking due to intermolecular hydrogen bonding and electrostatic interactions between the functional moieties of the constituents, contributes to the rigidity of beads, which further prevents the syneresis phenomenon. Moreover, the polysaccharide network of hydrogel achieves a significant hydrophobic nature, which develops resistance to swelling behavior. The kinetics of swelling behavior and leaching of contents from the alkoxysilane modified and enzyme immobilized beads was investigated (Saitoh et al., 2000). Biohybrid beads with silica-polysaccharide matrix impart mesoporosity with integrated features of hydrogels and sol-gel lattices. Noble metal nanoparticles are high-efficiency catalysts (Burda et al., 2005; Astruc et al., 2005) and here palladium nanoparticles facilitate the silicate modification of polymer. Catalytic potential of the modified alginate beads is verified by glucose oxidation assay.



Scheme 4.1. Diagram showing the fabrication of chemically modified hydrogel beads.

Peroxidase enzyme decomposes the in vivo generated  $H_2O_2$  in natural systems, which has several thousand folds high turnover number. However, practical applications of the enzyme are subjected to certain demerits; it is extremely sensitive to environmental conditions, and has low operational stability. Therefore, the biocatalyst has been replaced by a highly efficient chemical catalyst or a well known peroxidase mimic, the homogeneous suspension of polyethyleneimine (PEI) based Prussian blue nanoparticle (PBNPs), to overcome the stability related issues and also it is an economically viable alternative. In this study the PBNPs are used as catalyst to decompose in-situ produced hydrogen peroxide during the glucose oxidation reaction (Jv et al., 2010), which is detected calorimetrically by two reaction pathways (a) redox conversion of 3,3,5,5, tetramethylbenzidine (TMB) to its oxidised form ( $TMB_{ox}$ ) on reduction of  $H_2O_2$ , (Jv et al., 2010; Lin et al., 2013) and (b) the formation of a derivative dye quinoneimine, on reaction between 4-aminoantipyrine and para-hydroxybenzoic acid in the presence of  $H_2O_2$ . Therefore, the findings in this chapter are focused on understanding the effect of alkoxy silane modification on the properties of alginate hydrogel in fabricating microscaled enzyme carriers, and on investigating the catalytic activity of encapsulated enzyme.

## **4.2. EXPERIMENTAL**

### **4.2.1. Materials**

Sodium alginate, potassium tetrachloropalladate ( $K_2PdCl_4$ ), 2-(3,4-(epoxycyclohexyl) ethyltrimethoxysilane (EETMS), polyvinylpyrrolidone (PVP), luminol, potassium ferricyanide, polyethyleneimine (PEI) were purchased from Sigma Aldrich. Glucose, 3,3,5,5-tetramethyl benzidine (TMB), 4-amino antipyrine, 4-hydroxybenzoic acid were obtained from Merck, and

anhydrous calcium chloride ( $\text{CaCl}_2$ , analytical reagent grade). Double distilled water was used for all the preparations.

#### **4.2.2. Preparation of PdNPs functionalised microscaled enzyme carrier**

Gel beads with homogeneous contents were prepared on cross-linking with  $\text{Ca}^{2+}$  ions. The colloidal dispersion of PdNPs was mixed with 8 mg/mL sodium alginate solution, along with the simultaneous addition of 1.0 mg/mL glucose oxidase solution. The solutions were supplied in a feeding ratio 2:1:1, a mixture of alginic acid, PdNPs, and GOx. PdNPs were prepared as reported in our previous findings and also in chapter III by rapid conversion of  $\text{Pd}^{2+}$  to  $\text{Pd}^0$  using EETMS as reducing agent in the presence of PVP as a stabilizer. The obtained polysaccharide-silica hydrogel is transformed into microscaled structures or beads. Each drop took the form of gel-like rigid spherical beads on treating with calcium chloride solution (8 % w/v) using a syringe.

Prussian blue nanoparticles (PBNPs) used for the study were synthesized using polyethyleneimine (PEI) as discussed in our previous reports. A typical procedure involves the addition of 0.285 mL of PEI (0.1 g/mL) to 1 mL solution of potassium ferricyanide (50 mM) under stirring conditions, followed by the addition of 0.142 mL of conc HCl to the solution. Deep blue color suspension of PBNPs was obtained on incubating the mixture at 70 °C for 4-5 h.

#### **4.2.3. Measurements of swelling, leaching, and mechanical properties**

The kinetics of swelling was studied by installing four sets of experiments, first three with variable concentrations of EETMS (2.5, 1.2 and 0.1 M) and one control experiment. Each set with 10-12 beads, dipped in 1 mL of distilled water. The beads were weighed every 24 hours, on

a regular basis for 15 days. The obtained values were averaged for all the beads. Similarly, the leaching behavior of the gel beads was studied.

#### **4.2.4. Characterization of enzyme carrier system**

The morphological study of nanoparticles was done by using transmission electron microscopy (TEM; Technai G2, 20 TWIN 50/60 Hz 210-240 V, 943205022121, the FEI Czech Republic with accelerating voltage 200 kV). Colorimetric analyses were done by using UV spectrophotometer (Hitachi U 2900, Hitachi Hi-Tech technologies, Tokyo Japan.). Luminescence studies were done by Fluorescence spectrophotometer (Hitachi F-7000, Hitachi Hi-Tech, science corporation Tokyo, Japan). Measurements were done in 1 cm quartz cuvette in the wave length range of 200–700 nm. Dynamic light scattering (DLS) investigations were done using Malvern particle size analyzer instruments. The Young's modulus was measured using the Rheometer Expansion system. The topographical features of beads were evaluated using (scanning electron microscopy) SEM, ZEISS Oxford Instrument S1-ADD0048. TGA/DTA measurements were done using Perkin Elmer STA-6000 thermal analyzer, USA.

#### **4.2.5. Glucose oxidation and peroxide decomposition reaction**

Typical process of glucose oxidation is carried out as: a series of experiments were set up using eppendorf tubes (1.5 mL), with glucose over the range of 10 mg/dL to 1000 mg/dL. Two beads were fed into each tube containing 0.1 mL of glucose solution and incubated for 5-10 min. Beads were isolated and transferred to next set of experiment after washing. The in situ generated H<sub>2</sub>O<sub>2</sub> acted as substrate for TMB oxidation and also the formation of quinoneimine. A solution of TMB (10 μL, 5mM) and PBNPs (10 μL) were added to each of the tubes and the contents were

mixed. Similarly, another assay involves the addition of a mixture of 4-hydroxybenzoic acid and 4-aminoantipyrine to the filtrates from the first step of the reaction, followed by the addition of PBNPs (10  $\mu$ L). The appearance of pink color in all the tubes, with intensity depending on the concentration of glucose supplied and the corresponding amount of  $H_2O_2$  generated, confirms the formation of derivative dye quinoneimine.

### 4.3. RESULTS

#### 4.3.1. Measurement of interactions between the functional moieties

The stability of electrostatic interactions amid the functionalities of constituent molecules was studied using zeta potential measurements. The z-potential determines the charge on the systems, which gives an idea of probable interactions between the residual groups (-COOH/-NH<sub>2</sub>/-OH). For this reason, the z-potential of GOx and EETMS functionalized PdNPs modified and unmodified alginate solutions were determined.

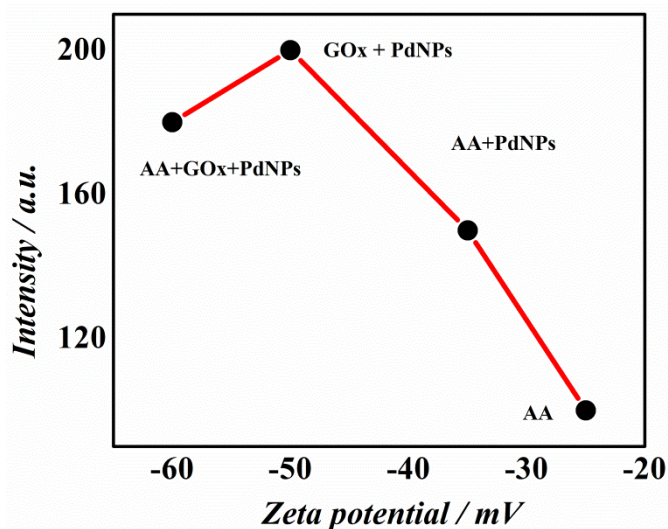


Figure 4.1. Variation in zeta potential of different unmodified (AA) and modified alginate solutions; AA + PdNPs, AA + GOx PdNPs.

Both the modified and unmodified systems possess negative value of zeta potential. The highest negative value ( $\sim -60$  mV) was obtained for the mixture (GOx-PdNPs-AA), which shows the extent of stability of interactions between the constituents. The z-value for bare sodium alginate solution is quite low than the modified systems ( $\sim -25$  mV). Owing to the acidic nature of the polymer the residual carboxylic groups on polysaccharide remain protonated (Zhang et al., 2016) and hence possess low negative charge. The encapsulation of PdNPs in the polysaccharide matrix led to the increase in z-potential value ( $-37$  mV), while on mixing glucose oxidase (GOx) enzyme with PdNPs increased the z-potential to even higher negative value ( $\sim 48$  mV). PdNPs are negatively charged due to the presence of diffused layer of counter  $\text{Cl}^-$  ions in the colloidal solution. Thus the z-potential values are elevated on the introduction of PdNPs into the matrices of alginate polymer and enzyme (GOx). The increase in negative value shows the system became progressively stable on mixing the constituents at each stage. This attributes to the enhancement in intermolecular interactions between the organic functionalities of the corresponding additives.

#### **4.3.2. Synthesis of biohybrid hydrogel**

Alginate matrix is rationally tailored (Tran et al., 2011; Hosoya et al., 2004) with alkoxy silane functionalized palladium nanoparticles (Figure 4.2) suspension to generate a three-dimensional architecture, which supports the homogenization of contents, while hindering the agglomeration it also prevents the leaching of nanoparticles. Such robust properties of the polysaccharide-silica matrix promote the encapsulation of macromolecular cargo (glucose oxidase). Surface modification of the alginate polymeric framework could further enhance the interactions between pore channels and the enzyme, which might greatly influence the stability and catalytic performance. Scheme 4.1 illustrates the overall steps involved in the fabrication of enzyme



carrier system. The secondary hydroxyl groups attached to alginate polymer behave as linkers for silanol groups via sol-gel processing. Other organic linkers like carboxylate groups act to strengthen the cross-linking by dimer formation (Gdaniec et al., 2003) via intermolecular hydrogen bonding as illustrated in Scheme 4.3. Alternate hydrogen bonding assemblies of carboxylic acid dimer form the continuous backbone of the silica-polysaccharide matrix.

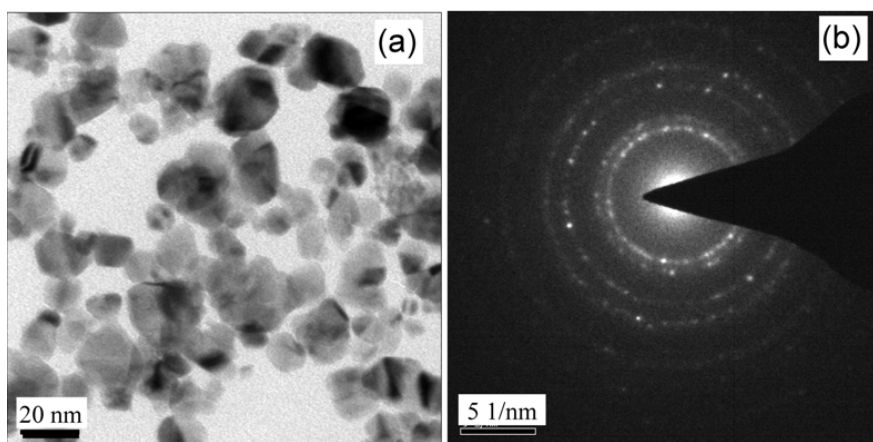


Figure 4.2. (a) TEM image, (b) SAED pattern of Palladium nanoparticles.

---

Dynamic light scattering studies were carried out in order to understand the possibility and extent of cross-linking between the constituents of modified beads in terms of hydrodynamic radii ( $R_H$ ). The  $R_H$  value of unmodified alginate hydrogel (145.8 nm) and corresponding silica modified hydrogel at several stages of feeding the additives (PdNPs/EETMS) is measured as, 112.4 (0.01 M), 105.7 (0.5 M) and 68 dnm (2.5 M) (Figure 4.3). The decrease in radius in the presence of silane moieties, credits to cross-linking between the residual groups of polysaccharide (Park et al., 2008) and alkoxy silane (Peng et al., 2016). Owing to the tendency of organosilanes to undergo hydrolysis and condensation via sol-gel processing (Tran et al., 2011), the hydroxyl

groups of polysaccharide at C2 and C3 condense with the silanol groups of organosilane (Gdaniec et al., 2003). It might be connecting parallel or randomly overlapping chains of polysaccharides through Si – O – Si linkage. The specific interactions were further analysed by infrared spectroscopy, where IR spectra (Figure 4.4) of modified alginate hydrogel shows a sharp band at  $1066\text{ cm}^{-1}$  which acknowledges the –Si – O – stretching vibration.

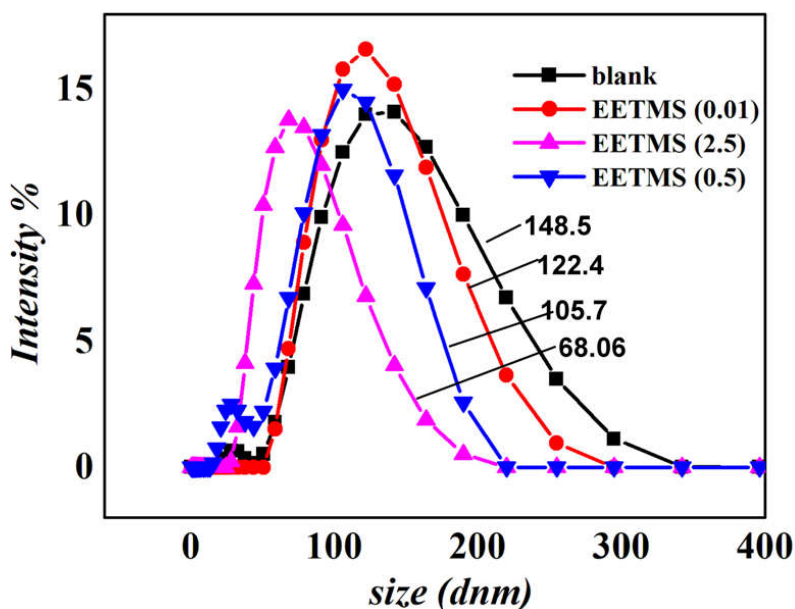


Figure 4.3. Hydrodynamic radii of alginate polymer solutions at different stages of modification using different concentrations of organosilane [2-(3,4 (epoxycyclohexyl)ethyltrimethoxysilane (EETMS)].

The characteristic broad signal at  $3522\text{ cm}^{-1}$  is responsible for the free hydroxyl group (Gdaniec et al., 2003), and signal due to hydroxyl moiety of the carboxylic group expected at  $3332\text{ cm}^{-1}$  is merged into this broad signal (Figure 4.4).

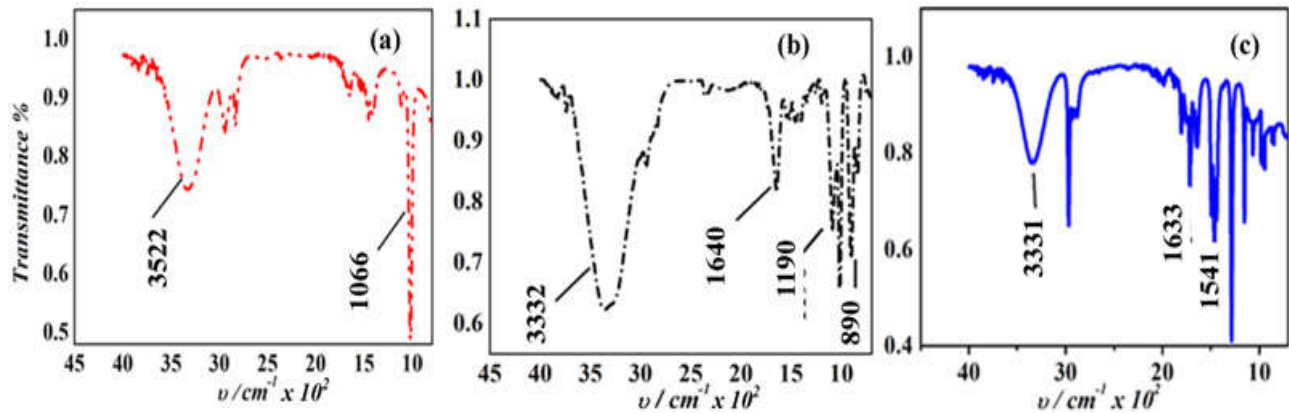


Figure 4.4. (a) FTIR spectra of alginate hydrogel alone, (b) alginate hydrogel with alkoxyfunctionalized palladium nanoparticles and (c) spectra of silica modified alginate hydrogel encapsulated with glucose oxidase enzyme, with peaks at 1653 and 1541  $\text{cm}^{-1}$ , referring to the IR stretching bands of amide I (C=O) and amide II (N-H and C-H).

### 4.3.3. Moulding of enzyme carrying unit

The role of alkoxyfunctionalized silane (EETMS) in fabricating a biocompatible and functional enzyme carrier system is investigated. Alkoxyfunctionalized silane in the form of palladium nanoparticle dispersion is mixed with alginate hydrogel to form a mesoporous silica-polysaccharide matrix. This mesoporous phase is formulated while simultaneously encapsulating the glucose oxidase (GOx) enzyme within the mesoporous domains (Chang et al., 1996). Enzyme gets entrapped into the cross-linked domains of the modified hydrogel. On treatment with calcium chloride (Thu et al., 1996), this silica modified hydrogel is transformed into spherical homogenized and micro-sized biohybrid beads, using fine rapid injection technique at a transfer rate of 50 beads/sec.

This technique ensures the homogenous distribution of the contents and generates the beads with uniform dimensions. 0.1 mL (4 mg) of enzyme solution was added to alginate hydrogel solution to achieve 0.5 mL total volume of the mixture. One micro-sized bead is formed nearly by 0.02

mL of mixture. Accordingly, each bead enclosed  $\sim 0.004$  mL of the enzyme, which is found to be sufficient for catalysing the conversion of 0.1 mL of glucose substrate in 5-10 minutes. Figure 4.5 shows the SEM micrographs of silica modified beads for controlling the porosity. Additionally, the immobilization of enzyme in silica functionalized framework of beads enhances the thermal stability of hydrogel.

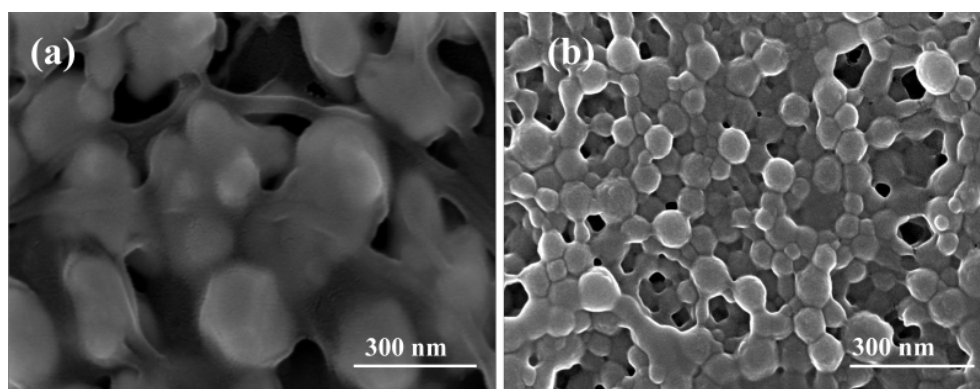


Figure 4.5. HR-SEM images of alginate hydrogel beads (a). Beads with (b) and (c) 0.01M EETMS, while (d) and (e) 2.5 M EETMS.

---

#### 4.3.4. Thermal decomposition

We observed that under inert atmospheric conditions, first mass loss for alginate hydrogel occurred at 94 °C, with onset temperature 52 °C (Figure 4.6), this is due to devolatilization of solvent (water). However, the definite decomposition of cross-linked polymer with divalent cations began at 140 °C with 13.2% weight loss. Corresponding DTA curve (Figure 4.6a) of the blank polymer shows a sharp endothermic dip at 123.47 °C. The total mass loss is relatively lower in case of silica modified and enzyme encapsulated alginate polymer as compared to the blank alginate polymer. Only 38 % of the sample (blank alginate polymer microspheres) was left over as residue, whereas 56 % of the residue of protein encapsulated polymer beads was left out.

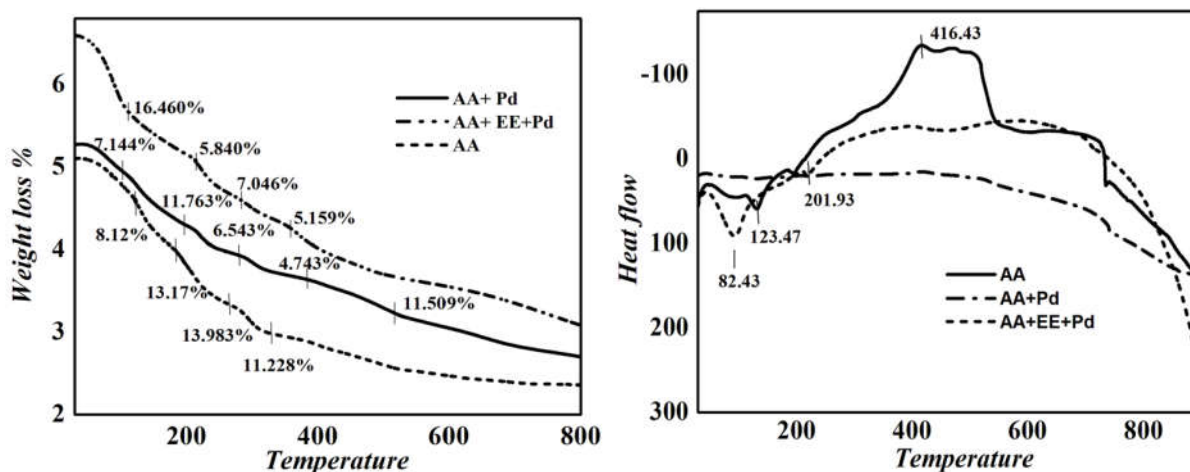


Figure 4.6. TGA (a) and DTA (b), curves for modified and unmodified alginate polymeric beads.

This confirmed the stability of GOx in constructed microscaled enzyme carrier system. The first and second stages are endothermic in case of all the variants and later stages are exothermic for pure alginate polymer and nanocatalysts modified samples. DTA thermogram of protein entrapped polymer matrix shows a finite endothermic dip at 82.43 °C, with the enthalpy change of 231.972 J/g, which attributes to the energy required for release of cross-linked water molecules. In contrast, a less distinguished endotherm at 43.50 °C is observed in case of alkoxysilane based palladium nanoparticle modified alginate polymer beads, the small peak height indicates the slow reaction (Thu et al., 1996).

#### 4.3.5. Glucose oxidase enzyme assay and subsequent peroxidase mimetic activity of PBNPs

As GOx encapsulated polymer beads are selective towards pH changes, it was observed that the fabricated biohybrid beads were able to effectively catalyze the cascade reaction, enzymatic

oxidation of glucose to yield gluconic acid and hydrogen peroxide ( $H_2O_2$ ) (Lin et al., 2013; Tatsuma et al., 1989). The catalytic action of biohybrid microscaled beads was studied over successive experimental cycles for several weeks under different conditions (Peng et al., 2016). Initially, the stability of hydrogel-GOx-PdNPs mixture was examined at room temperature and  $4^\circ C$  for several consecutive weeks including the overnight storage sessions at  $4^\circ C$  and the activity was recorded every 5 days. The activity of the free enzyme was far reduced than the immobilized one. Our findings show that enzyme rarely oozed out of the porous matrix within the mentioned time scale of the experiments.

Subsequent oxidation of glucose by GOx, gluconic acid (Tatsuma et al., 1989) was produced and the acidity of the solution was enhanced, and the  $H_2O_2$  (Pandey and Chauhan, 2012a; Pandey and Pandey, 2012b; Pandey and Pandey, 2013) produced is analyzed by luminescence intensity (Zhang et al., 2005; Robinson et al., 1999) using basic solution of luminol (Quickenden et al., 2001), which gets oxidized in the presence of peroxide ions (oxidizing agent) and emits spontaneous blue light (Figure 4.7). The recorded variations in the intensity of luminescence are the exact function of  $H_2O_2$  concentration, produced during first step of reaction. Further, the catalytic decomposition of  $H_2O_2$  is carried out using artificial peroxidase mimic, PBNPs. We have investigated the reduction of in situ generated  $H_2O_2$  via two different pathways: (1) TMB/ $H_2O_2$ /PBNPs and (2) quinoneimine/  $H_2O_2$ /PBNPs (Lin et al., 2013; Mba et al., 2008; Deng et al., 2014). The oxidation of TMB using  $H_2O_2$  in the presence of PBNPs as catalyst is largely a function of pH, as PBNPs get self activated under acidic conditions thus, increased acidity can enhance the rate of oxidation of TMB.

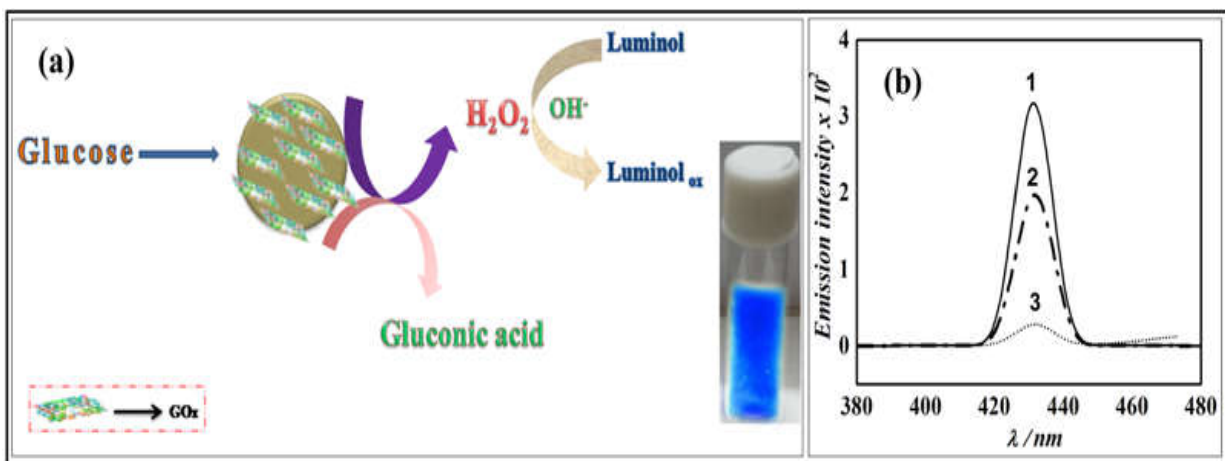


Figure 4.7. (a) Schematic illustration of catalytic activity of enzyme immobilised beads, (b) Luminescence spectra showing the variation in absorbance, as a function of concentrations of enzyme (1) 6 mg, (2) 4 mg (3) 2 mg in 0.2 mL phosphate buffer.

Figure 4.8 shows the absorbance spectra of TMB oxidation, where the intensity of absorbance is observed to enhance with an increasing concentration of H<sub>2</sub>O<sub>2</sub>, which is supplied indirectly to the system. H<sub>2</sub>O<sub>2</sub> is generated in situ in the first step of reaction; enzymatic oxidation of glucose, which was studied as a function of glucose concentration over the range 10 – 1000 mg/mL. The proportionate volume of H<sub>2</sub>O<sub>2</sub> produced under respective concentrations of glucose worked as substrate for final stage of the reaction. The redox reaction between TMB and H<sub>2</sub>O<sub>2</sub> in the presence of PBNPs was monitored colorimetrically. UV-Vis spectra in Figure 4.8 show the change in absorbance with respect to the ratio of H<sub>2</sub>O<sub>2</sub> present in a particular set of reaction. The appearance of greenish blue color with two characteristic peaks at 370 and 660 nm, (Figure 4.8a) shows the reaction was incomplete, but as soon the pH was brought to unity, emergence of characteristic yellow color denoted the complete oxidation of TMB and the absorbance maxima was shifted to ~385 nm (Figure 4.8b).

Similarly, in another reaction pathway a mixture of 4-aminoantipyrine and p-hydroxybenzoic acid were supplied in equimolar ratio to the reaction set up. The quick emergence of pink color (Figure 4.9) on addition of PBNPs and the appearance of characteristic peak at 527 nm in visible spectrum, confirms the formation of quinoneimine which is a derivative dye with resonating quinonoid structures. The calibration plot of absorbance versus amount of glucose supplied (Figure 4.9b), was found to be linear over the range of concentration of glucose from 10 mg/dL to 1000 mg/dL.

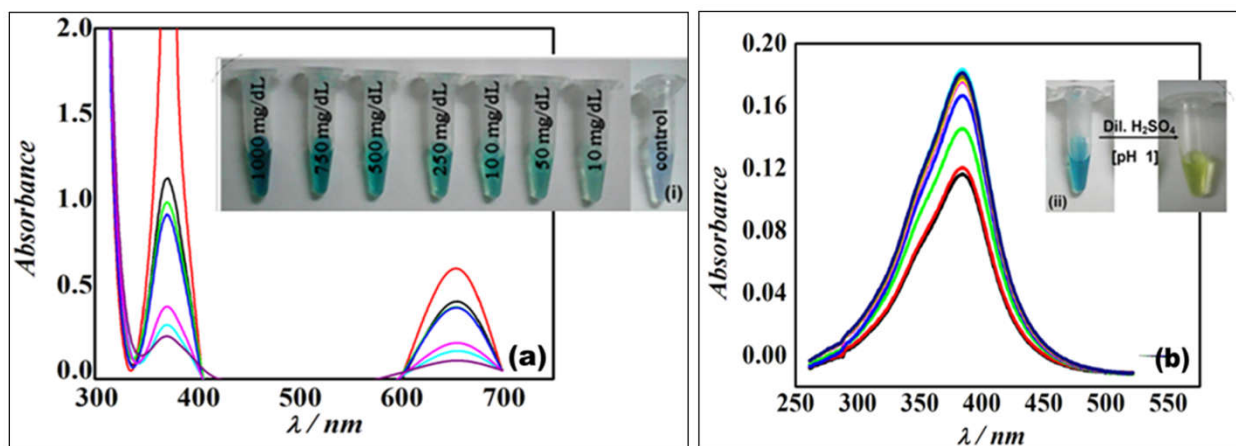


Figure 4.8. Colorimetric detection of oxidation of TMB in the presence of Prussian blue (PBNPs) nanoparticles. (a) Concentration dependent absorbance of TMB at 650 nm in different reaction systems. (b) Characteristic peak at 370 nm at pH = 1 of the reaction medium. Inset pictures (i) variation in color of reaction medium, (ii) appearance of yellow color upon addition of acid.

## 4.4. DISCUSSION

### 4.4.1. Electric properties of system

The electric interactions between the encapsulated protein, alkoxy silane moiety and the alginate polymer are used as a major building block to fabricate the hydrogel beads influences the



retention of enclosed molecule. The  $\text{-COOH}$  groups on polymeric chain and enzyme molecules, in protonated form lead to inter and intramolecular hydrogen bonding with the silanol groups of alkoxy silane,  $\text{-OH}$  groups and  $\text{-COOH}$  groups on parallel or randomly oriented polymeric chain or enzyme molecules, while in carboxylate form ( $\text{-COO}^-$ ), it undergoes electrostatic interactions (repulsive and attractive) with those of  $\text{-NH}_3^+$  groups. Thus, highest magnitude of z-potential for the mixed system defines the extent of interactions between the concerned moieties, which has been explored further as discussed later in the chapter.

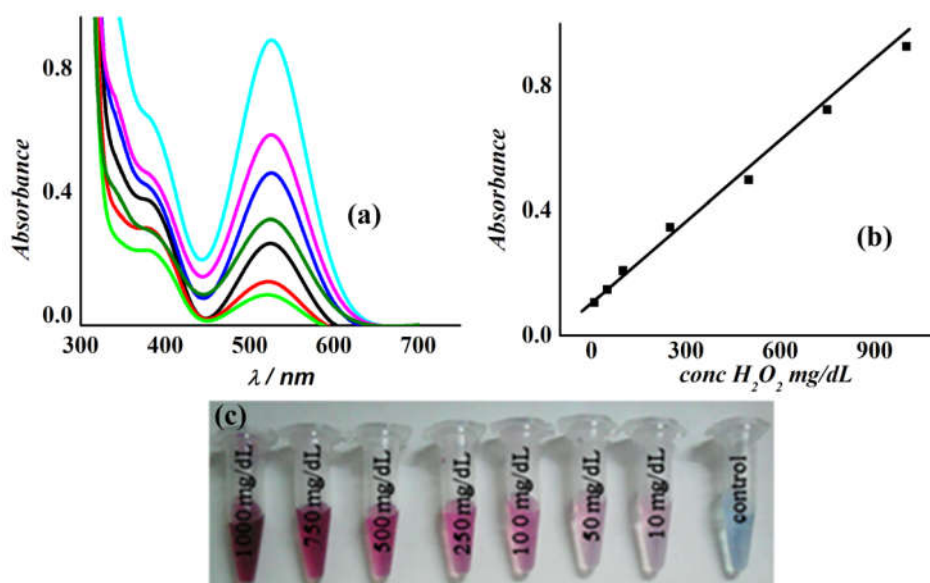
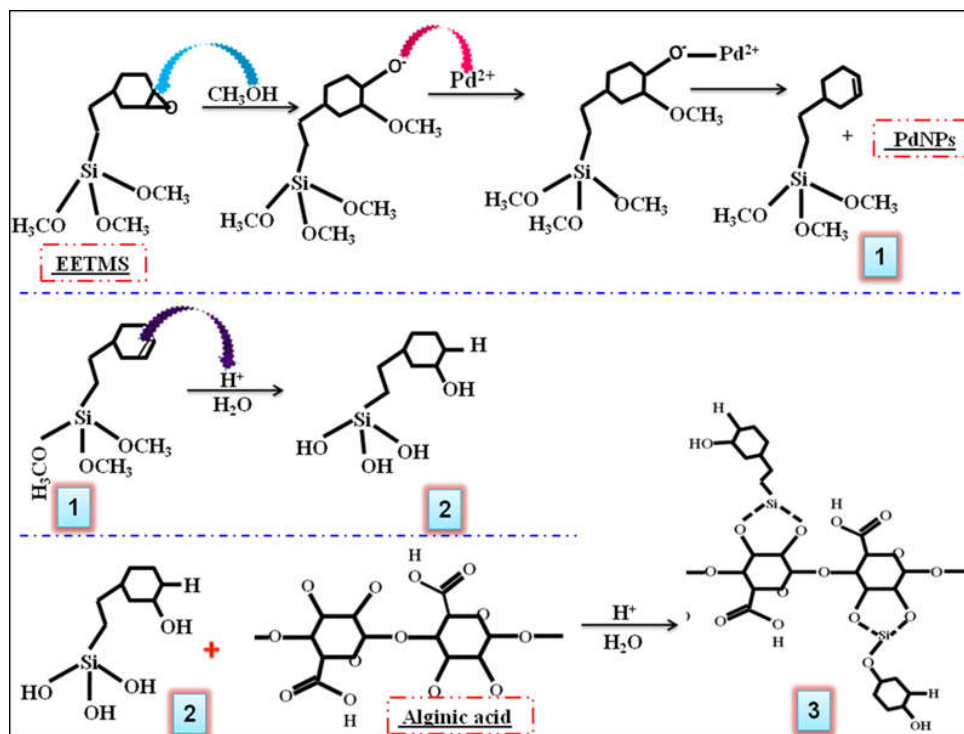


Figure 4.9. Colorimetric detection of formation of quinoneimine in the presence of Prussian blue (PBNPs) nanoparticles. (a) Concentration dependent absorbance 527 nm in different reaction systems. (b) Corresponding calibration plot of absorbance Vs concentration of glucose, (c) picture shows the variation in color as a function of concentration of glucose.

#### 4.4.2. Preparation of Biohybrid precursor

Introduction of alkoxy silane functionalized palladium nanoparticles (Scheme 4.2) into the concentrated solution of alginate polymer, led to the shift in FTIR signal to  $3331\text{ cm}^{-1}$ , which is

probably because the carboxylate groups of two linear or randomly oriented polysaccharide chains undergo intermolecular hydrogen bonding to form the carboxylic acid dimer (Scheme 4.3). Further, the epoxy moiety of EETMS is subjected to electrostatic interaction with residual functional groups of polysaccharide matrix. Addition of lipophilic domains subsequently enhanced the hydrophobicity of the support material (Underhill et al., 2002). The degree of hydrophobicity is measured in terms of wetting and dewetting of the surface (Ogihara et al., 2012), which is deduced by contact angle measurement. The hydrophilic nature of alginate hydrogel (Lee et al., 2000) with contact angle below  $10^\circ$  is rationally transformed to slight hydrophobic character, in order to enhance the catalytic activity. This prevents the passive solubilization and leaching of contents (Draget et al., 1996). Although the contact angle of exposure to aqueous substrate solution in case of the modified hydrogel is increased, microsized spherical beads are acting as a heterogeneous catalyst. The EETMS shows characteristic signals at  $2920\text{ cm}^{-1}$  from C–H stretch of alkyl groups while bands at  $1190$  and  $890\text{ cm}^{-1}$  from –C–O–C– stretching vibration of the epoxide ring unit attached to cyclohexyl moiety of alkoxy silane. At low EETMS (0.1 M) characteristic signal at  $1640\text{ cm}^{-1}$  from –C=C– stretch is observed, giving a clear evidence of olefin moiety (Figure 4.4), while signals at both  $1640$  and  $1190, 890\text{ cm}^{-1}$  are recorded at relatively higher the EETMS (2.5 M) concentration. This means at a higher concentration of EETMS there is a possibility of the presence of untransformed epoxy cyclohexyl moiety. The bands due to olefinic and epoxide moieties disappear, on introducing the palladium nanoparticle dispersion containing a high concentration of EETMS into alginate hydrogel matrix. The double bond might possibly undergo electrophilic addition (Boyd et al., 2005), while the opening of epoxide ring is promoted in acidic conditions (Darensbourg et al., 2003).



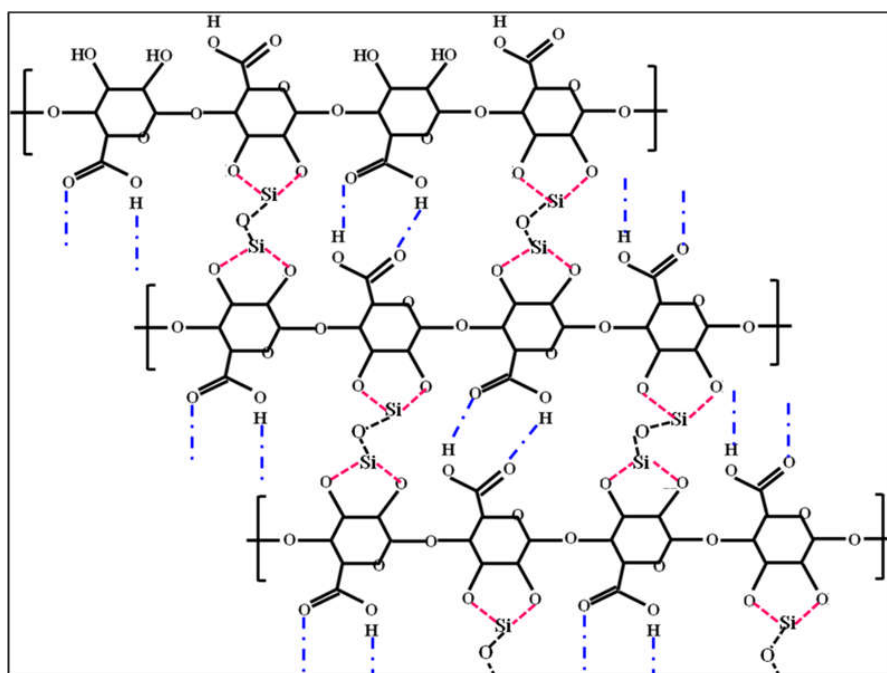
Scheme 4.2. Possible mechanism of organosilane induced conversion of  $\text{Pd}^{2+}$  to  $\text{Pd}^0$  and combination of byproducts of EETMS with alginate.

Resulting monohydric and dihydric alcohol derivatives of EETMS also participate in strengthening the cross-linking between the polymeric chains and alkoxy silanes, to successfully synthesize tunable polysaccharide-silica hydrogels. The degree of cross-linking and pore diameter was precisely controlled by regulating the viscosity of the mixture (Tran et al., 2011) and the concentration of EETMS.

#### 4.4.3. Fabrication of PdNPs functionalised microscaled enzyme carrier

The treatment of as obtained alkoxy silane functionalized biohybrid hydrogel, with multivalent cations ( $\text{Ca}^{2+}$ ) led to the formation of microsized spherical structures. The globular bead like assembly of hydrogel with improved rigidity and porosity, on the whole acts as enzyme carrier.

The fine pore channels of the carrier allow the enhanced accessibility of the substrate molecules to the active sites on its surface. Further, such enzyme carrier systems facilitate the use of GOx over iterative experimental cycles and hence retain its catalytic activity. Additionally, the immobilization of enzyme in silica functionalized framework of beads ensures the thermal stability as discussed later in the chapter.



Scheme 4.3. Schematic representation of the probable cross-linking between the residual functional groups of enzyme with those of fabricated polysaccharide-silica matrix.

---

#### 4.4.4. Role of Palladium in fabrication of enzyme carrying unit

An attempt has been made to understand the role of palladium during the formation of silica-alginate beads. The observations demonstrated the following; (i) EETMS is not homogeneous with alginic acid solution, (ii) reactivity of epoxy-functionality may ultimately yield into a reactive bead. However, our recent finding exhibited a specific interaction of EETMS and

palladium cations that favors the formation of palladium nanoparticles stabilized through by-product of EETMS. As generated Pd-EETMS sol is found to homogenize with the polymeric matrix to yield silica-alginate beads and enable the direct cross-linking between the residual groups of organosilane and polysaccharide. Our findings reveal that the presence of palladium nanoparticles within silica-alginate beads enhances the biocompatibility and amplifies the stability of beads for practical applications as compared to that the same in absence of palladium nanoparticles. Additionally, it reinforces the ease of immobilizing the macromolecular cargo.

#### **4.4.5. Thermogravimetric analysis and stability of carrier**

Temperature elevation introduces variations in physical and chemical properties of the alginate polymer composites. Thermal decomposition of polysaccharides, in general, includes following distinct phases: (i) dehydration, (ii) depolymerization and (iii) development of polynuclear aromatic structures (Hajighasem and Kabiri, 2013; Grabowska et al., 2017; Pramoda et al., 2005). The hydroxyl groups of polymeric chain with those of silanol groups of form hydrogen networks, which lead to the formation of small crystallites. DTA curves for, alkoxysilane modified, enzyme encapsulated and pure alginate polymer beads, display the consistent characteristics features with those of TGA results. The exothermicity observed means that the energy released from burning or forming new chemical bonds was greater than the energy absorbed for bond scission during decomposition. In case of pure alginate samples, the relatively higher rate of decomposition is observed in the temperature range 140-380 °C, with ~ 42 % loss in weight (Hajighasem and Kabiri, 2013).

Within this range, glycosidic linkages between guluronate and mannuronate monomeric units decompose and polymeric chains transform into shorter ones. This is followed by a slower rate of decomposition within the thermal range 390-500 °C, where the intermediates (metal alginate) are converted to gaseous products, thereafter certain inorganic compounds generated start to decompose at ~800 °C. In the oxygen-free atmosphere, decomposition of alkoxy silane modified polymer gel beads with and without GOx, occurs in several stages (4-6 mass losses) (Figure 4.5). The rate of decomposition is slow and shifted towards higher temperatures. This might be due to the cross-linking network formed by the inclusion of organosilane moieties, which promoted various inter and intramolecular interactions such as Si-O-Si linkages via sol-gel processing and formation of several polynuclear structures.

DTA curve of alkoxy silane modified beads, both in presence and absence of protein encapsulation does not show any significant exothermic effects, instead, few broad endothermic peaks accompanying pyrolysis do exist. The relatively greater amount of residue in case of the alginate polymer blank beads in contrast to the GOx loaded beads, justifies the amplified encapsulation efficiency of glucose oxidase in alkoxy silane modified alginate polymer matrix. Comparative study reveals that in the case of alkoxy silane based nanocatalysts modified alginate polymer beads entrapping glucose oxidase, the residue at 250-320 °C accounts for 70 % of the initial mass (Hajighasem and Kabiri, 2013; Grabowska et al, 2017; Pramoda et al, 2005; Pramoda et al, 2003). According to our results; the reason for the enhanced thermal stability is probably the introduction of organosilane based palladium nanomaterials in the polymer mixture. This further supports the enhanced catalytic potential of the enzyme immobilized system.

#### 4.4.6. Rheological properties of silica alginate beads

The storage modulus of the beads is measured as a function of the concentration of organosilane (EETMS). Time-dependent variation in the formation of a three-dimensional network of the cross-linked structure is represented in Figure 4.10. At higher concentrations of EETMS (2.5 M), a significant increase in  $G'$  is observed with time, while at the lower content of organosilane, relatively constant values of  $G'$  are recorded over time. The maximum strength of gel beads was obtained at  $\sim 450$  min. The amplified magnitude of storage modulus indicates the strong interaction forces among the constituents of the modified assembly of beads. It is observed that storage modulus of beads with high cross-linking i.e, with greater EETMS concentration, is altered significantly.

We note that the relation between storage modulus and EETMS concentration seems to vary depending on the experimental conditions at a constant amount of calcium. In general, gel swells due to the external pressure of solvent, but on chemical modification using alkoxy silanes moieties, such ordinary gains in entropy are reduced (Davidovich-Pinhas and Bianco-Peled, 2010). A linear relationship between the EETMS concentration and the degree of polymerization gives an independent estimate of cross-linking between the residual groups of GOx, alkoxy silane and alginate polymer. In order to assess the mechanical stability of the enzyme immobilized beads is estimated. Increasing the EETMS concentration facilitates the reduction in swelling ability, and also mechanical strength. Evidently, at higher EETMS concentrations there are higher coupling divisions. This shows the greater associations between polymeric chains and the alkoxy silanes moieties that could decrease the chain flexibility. Consequently, a lesser degree of swelling is achieved.

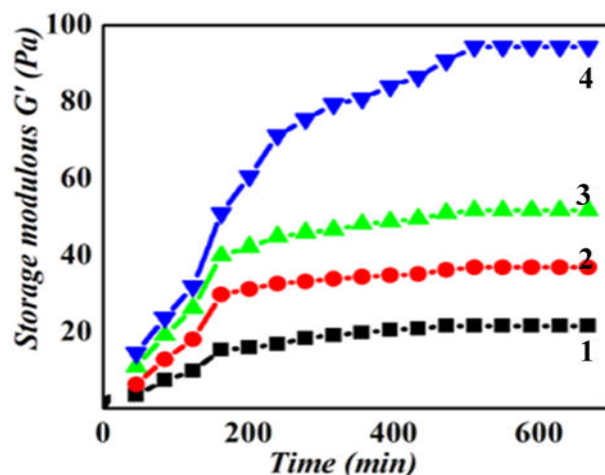


Figure 4.10. Evaluation of storage modulus at different concentrations of EETMS from (1-4).

#### 4.4.7. Enzymatic conversion and H<sub>2</sub>O<sub>2</sub> decomposition

The activity of the enzyme was estimated by varying the enzyme concentration several folds, per 100  $\mu$ L of glucose, as the amount of H<sub>2</sub>O<sub>2</sub> produced is proportional to the enzyme as well as glucose concentration. Decreasing trend of emission intensity suggests the generation of reaction product (H<sub>2</sub>O<sub>2</sub>) is highly dependent on the availability of active sites of the enzyme. Using Beer-Lamberts law equation,  $A = \epsilon cl$  the concentration of H<sub>2</sub>O<sub>2</sub> as a function of enzyme concentration can be calculated by placing,  $\epsilon = 43.6 \text{ M}^{-1}\text{cm}^{-1}$ .

Prussian blue nanoparticles (PBNPs) suspension, being artificially designed robust peroxidase mimetic (Jv et al., 2010; Ellis et al., 2009; Wang et al., 2007; Sono et al., 1996; Pelosof et al., 2010) catalyzes H<sub>2</sub>O<sub>2</sub> decomposition. The average size of PBNPs was about 40-45 nm. Owing to their high dispersibility in an aqueous medium, they are often used as homogenous catalysts. Therefore, second step of enzymatic assay is homogenous catalysis involving PBNP as a homogeneous catalyst. Significant enhancement in the catalytic potential of artificial enzyme



carrier system and PBNPs (peroxidase mimetic) with different surface modifications has been demonstrated via typical catalytic reactions. Apart from the enzyme concentration, the size of the polymeric beads has a significant effect on the substrate's interaction with the available enzyme active sites. A comparatively concise version of the beads was found to be catalytically more potent due to enhanced exposure of reactant molecules with those of enzyme.

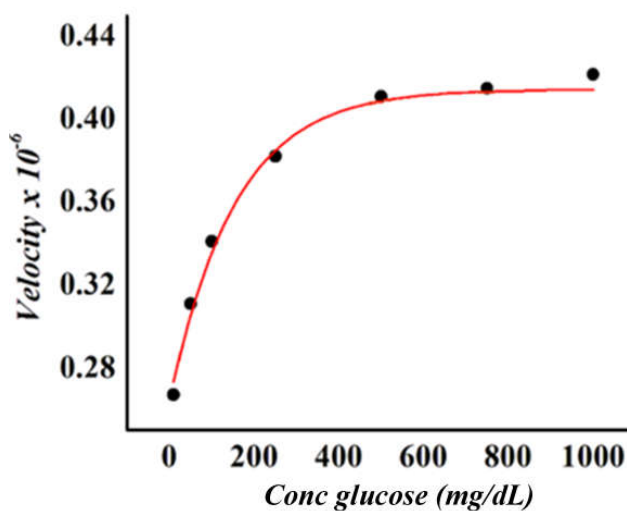


Figure 4.11. Kinetic analysis of PBNPs activity with in situ generated H<sub>2</sub>O<sub>2</sub> as substrate.

---

The value of  $K_m$  obtained to be 200 mg/dL or 11.11 mmol/L (Figure 4.11) which is higher as compared for those systems reported in the literature (Jv et al., 2010; Lin et al., 2013). A linear relationship was obtained between the rate of production of H<sub>2</sub>O<sub>2</sub> and the size of carrier system. There are two substrates in the reaction TMB and H<sub>2</sub>O<sub>2</sub>, thus the rate of reaction must be governed by the concentrations of both. Keeping the concentration of in situ generated H<sub>2</sub>O<sub>2</sub> constant, the variation in absorbance was recorded as a function of the concentration of TMB. At the upper limit of TMB concentration, a rapid blue shift in wavelength was observed even in the pH range of 2.5 – 4, while at lower concentrations the reaction was complete at pH ~1.

#### **4.5. CONCLUSIONS**

The mesoporous framework of silica-alginate beads is a suitable support material for enzyme encapsulation. The fabrication of such biohybrid assembly involves a simple two-step straight forward process, which ultimately results in ordered pore structure with outstanding chemical stability. Introduction of alkoxy silane functionalized nanoparticles induces direct chemical cross-linking between residual functional moieties of alkoxy silane, alginate hydrogel, and the protein molecules (glucose oxidase). The hydrophilic alginate hydrogel is transfigured to relatively hydrophobic material on interaction with lipophilic domains of organosilane, in order to reinforce the enzyme carrying properties of polysaccharide matrix. Enzyme encapsulated beads are used as biohybrid catalyst for the conversion of glucose to hydrogen peroxide, which is further decomposed by a well known peroxidase mimetic, Prussian blue nanoparticles. These findings emphasize on the generation of materials with flexible properties of different aspects.